International Journal of Computers and Informatics (IJCI)
Vol. (5), No. (5)
IJCI
May 2026
المجلة الدولية للحاسبات والمعلوماتية
الإصدار (5)، العدد (5)

A Cost-Effective Framework for Transforming Conventional Microscopes into Intelligent Diagnostic Platforms using Systematic Multi-Field Acquisition Protocoland Multimodal LLMs

Noor Aldeen A. Khalid
Department of Medical Instruments Engineering Techniques, Bilad Alrafidain University College, 32001, Diyala, Iraq
Dr.nooraldeen@bauc14.edu.iq

Aymen A. Hameed
Department of Medical Instruments Engineering Techniques, Bilad Alrafidain University College, 32001, Diyala, Iraq
Draymen@bauc14.edu.iq

Ali Ismail Alwandi
Bilad Alrafidain University College, 32001, Diyala, Iraq
hamada.110011ali@gmail.com

Abstract

Urine and stool cultures under the microscope are a main method of diagnostic work, but manual analysis is not only dependent on experience of the examiner but also suffers visual fatigue and subjectivity. Although, automated systems are available, their cost is so high that they are not often integrated in resource-limited environments. In this paper,we proposes a MicroScan AI, a low-cost solution that will be used to convert a standard optical microscope into a smart platform capable of diagnostic tasks. Morphological reasoning is done by connecting a digital microscopic camera with ,a 0.5x reduction lens with multimodal Large Language Models (LLM), namely ChatGPT-4o Gemini, and Claude, and conducting the reasoning through encrypted API channels. A counting-methodology was used to counteract a 60% field-of-view (FOV) hardware-induced *aggregation* based field limit by a structured five-field acquisition scheme (F1–F5) scheme and Systematic Multi-Field for image pre-processing protocol . The validation of the experiment was done using 20 clinical specimens and 200 diagnostic parameters against expert human opinion. The system had an agreement rate of 97% with a Cohen Kappa coefficient of 0.94 which signifies an almost perfect agreement. Examination of the 3-percent discrepancy indicated that the error occurred in adjoining semi-quantitative grading frequencies and not resultant categorical detection errors. These results make MicroScan AI a scalable clinical decision support system that improves diagnostic consistency and decreases operator dependency without necessitating the complete replacement of hardware.

Keyword: AI-Powered Microscopy, Urinalysis, Field-of-view Multimodal LLMs, Digital Pathology, Prompt Engineering.

1. Introduction

Microscopic analysis of biological samples, especially urine and stool, is a classic gold-standard diagnostic test in medical laboratories across the world, which traditionally has been completely based on manual visual inspection by laboratory specialists [1], in which the diagnostic value of the test is greatly influenced by the cumulative experience, interpretation and visual acuity of the examiner. Although manual microscopy can play a vital role in clinical decision-making, it is not an exception, as prone to high levels of variability [2], located in the context of human factors including visual fatigue and lack of objectivity in high-volume conditions, manual microscopy inevitably results in inconsistency of reporting pathological findings, which in turn can affect patient care. As the digital world develops at an alarming pace, Artificial Intelligence (AI) has become a disruptive phenomenon in healthcare [3], as it promises to speed up the diagnostic process and provide the degree of analytical reliability and consistency by acting on the principles of standard algorithms that minimize the possibility of fatigue-related mistakes. Nevertheless, practical implementation of AI in everyday microscopy is highly hindered by the fact that modern commercial automated systems are prohibitively costly, difficult to use, demand a complete reorganization of the existing laboratory facilities, and are accompanied by a significant lack of training [4] of new graduates of laboratory technologists in the field who may lack the extensive work experience to observe small abnormalities or rare life stages of parasites.

To overcome them, the study proposes MicroScan AI, a framework with these features that allows optimizing the traditional laboratory business model by updating conventional optical microscopes with a hybridizing digital imaging and cloud-based multimodal Large Language Models (LLMs) [5] like ChatGPT-4o, Gemini, and Claude. With the help of polished reasoning capabilities of these engines, MicroScan AI turns raw visual data of the microscopes into patterned clinical information and serves as a Clinical Decision-Support Tool which gives structured findings in the form of Raw JSON data and confidence scores, to help the lab employees in their ultimate verification. The main purpose of the study is to design, implement, and test a smart microscopy system that improves consistency of the diagnostic process, is accessible in resource-limited settings, and its specific objectives include augmenting the hardware with a high-resolution digital interface [6], to enable real-time acquisition, and AI augmentation with the creation of an analytical layer in the form of software to analyze morphological features using multimodal LLMs, using encrypted API channels. Moreover, the research is concerned with the optimization of methods through the adoption of a multi-field acquisition scheme (F1–F5), counting-based aggregation to eliminate optical field-of-view mismatches and clinical validation by testing the system to performance on expert human consensus in a real-world laboratory setting to determine its reliability in analysis. MicroScan AI represents a scalable solution to the modernization of clinical diagnostics by connecting the manual environment of microscopy with the digital one, which helps employ the work of laboratory staff and minimizes the variability in examination depending on the examiner.

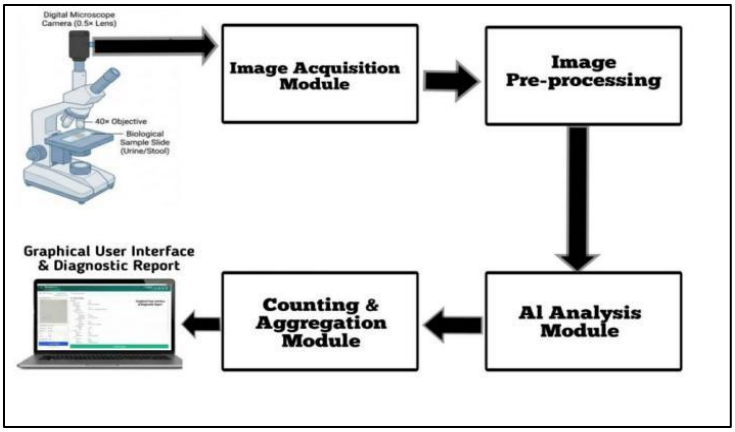

Fig. 1. MicroScan overview.

The MicroScan AI framework addresses the digital transition challenges identified by [7] who outlined major trends and hurdles in applying AI to pathology, prompting our development of a low-cost solution that overcomes the high cost of existing automated systems. This aligns with the "AIMIC" framework developed by [8], which successfully utilized deep learning for microscopic image classification; however, our project advances this by employing Multimodal LLMs for morphological reasoning rather than simple classification. Building on the foundational work of [9], who demonstrated that neural networks can fundamentally enhance optical imaging, MicroScan AI leverages similar principles to turn raw visual data into structured clinical information. Furthermore, [10] confirmed the effectiveness of AI-supported digital microscopy in primary healthcare laboratories through a scoping review, supporting our objective of making advanced diagnostics accessible in resource-limited settings. In specialized parasitology, [11] proposed an AI approach that successfully segmented human parasite eggs, and [12] developed an automatic recognition system for stool parasites with robust detection; these results reinforce our system's ability to achieve a 0% categorical failure rate in detecting pathogens. To ensure statistical rigor, we integrated the considerations of [13] on the Kappa statistic and the evaluation framework of [14], which allowed us to document a 0.94 Cohen Kappa coefficient, signifying almost perfect agreement. Our work is situated within the broader digital transformation of laboratory medicine reviewed by [15] and [16], who both highlighted how AI significantly improves diagnostic accuracy and consistency. Specifically, our use of integrated visual and textual data for reasoning echoes the findings of [17] and [18], who proved that multimodal AI like ChatGPT can revolutionize clinical workflows, contributing to our overall 97% agreement rate with experts. While [19] achieved advanced imaging through complex multi-camera arrays, we successfully addressed hardware-induced field-of-view limitations (60%) via a more accessible software-based five-field (F1–F5) acquisition strategy. This focus on automation is further validated by [20], who developed an intelligent scanner that significantly increased tuberculosis detection accuracy and reduced misdiagnosis, paralleling our goal of eliminating errors caused by manual examination fatigue. Finally, as [21] demonstrated the

superiority of digital pathology over conventional microscopy, we addressed the pitfalls of whole-slide analysis identified by [22] and the data quality requirements stressed by [23] and [24] by implementing a high-resolution digital interface and a consensus-based grading protocol, mirroring the precision seen in the ISE-YOLO model for blood cell detection by [25]. In this paper, we utilize the MicroScan AI system, which is a low-cost system that is used to augment the traditional optical microscopes into smart diagnostic systems. We use the capabilities of multimodal Large Language Models (LLMs), namely ChatGPT-4o, Gemini, and Claude, to do advanced morphological reasoning on clinical samples using encrypted API channels. In order to resolve the 60 percent field-of-view restriction that is introduced by hardware, our research design adopts a systematic five-field (F1–F5) acquisition scheme and a counting-based aggregation model to guarantee clinical representative sampling. We create a scalable clinical decision-support tool, which can improve the consistency of diagnosis and minimize reliance on manual examination by converting raw microscopic imagery into structured data in the form of JSON and confidence scores. The remainder of this paper is organized as follows: Section 2 details the Methodology, covering the integrated system architecture, hardware configuration, the AI-driven analytical framework with specialized prompt engineering, and the computational aggregation and statistical methodology. Section 3 presents the Results and Discussion, providing an in-depth analysis of diagnostic concordance, statistical performance metrics such as Cohen's Kappa, and the effectiveness of hardware constraint mitigation strategies. Section 4 provides the Conclusion, which summarizes the core findings regarding the system's reliability and the clinical implications of the MicroScan AI framework in modernizing laboratory diagnostic

2.Methodology

2.1 Integrated System Architecture and Hardware Configuration:

The MicroScan AI system is developed and innovated as a multilayer diagnostic ecosystem with a deep ontology created specifically to overcome a wide technological chasm between the conventional manual microscopy and the high-end digital pathology branches. The design ideology of this model is based on the concept of modular augmentation that highlights the cost-efficient enhancement of the current laboratory facilities instead of full replacement.

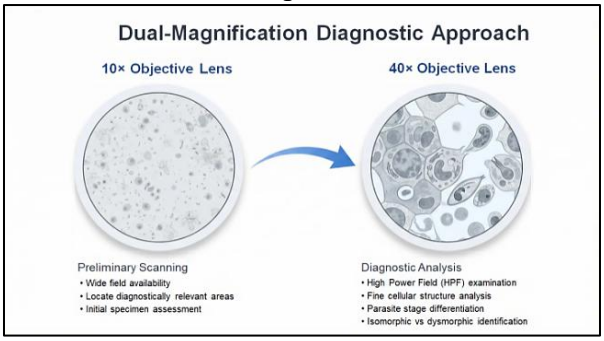

Fig. 2. MicroScan AI system architecture overview showing the three interdependent functional domains: Hardware Layer, Processing Layer, and Intelligence Layer.

This method is especially crucial to the medical laboratories that are operating under the constraints of the resources, since the steep price tag of the fully automated diagnostic platforms in most cases denies them a chance to implement the modern artificial intelligence possibilities. The system architecture is designed to have three functional domains that are interdependent on each other, which are the physical Hardware Layer, intermediary Processing Layer and the cloud-integrated Intelligence Layer, all in contact with each other to convert a traditional analog microscope into an intelligent diagnostic tool. The system has a physical basis that is the standard laboratory light microscope that is the universal gold standard of clinical urinalysis and fecalysis. In order to ensure maximum compliance with any conventional medical workflow, the microscope is used in its original design, preserving its capacity to be inspected manually concurrently by people working in the laboratory. The system applies a dual-magnification approach that secures evaluation of all specimens. The 10× objective lenses are used in preliminary scans availability of the wide field to enable the system or the operator to locate the diagnostically relevant areas of interest throughout the glass slide. Diagnostic analysis, however, takes place at the level of High Power Field (HPF) with 40× objective lenses. This magnification is necessary to both analyze the fine details of cellular structure, differentiate between isomorphic and dysmorphic erythrocytes, and distinguish between different stages of parasites like cysts as illustrated in Figure 2.

The optical arrangement is such that the visual information retrieved as a high resolution so that it can be processed by the artificial intelligence models to provide the complex morphological reasoning, which resembles the visual sharpness of a trained human expert. A high-resolution digital microscopic camera attached to the ocular tube of the microscope makes this transition possible from an analog optical image to a digital piece of data. This is a non-invasive form of integration that uses the eyepiece port, or a trinocular tube, to position the camera sensor along the optical axis of the microscope without making any long-lasting mechanical changes to the equipment. The lens adapter reduction of 0.5x is a paramount feature in this interface because it is the optical bridge that focuses the magnified image in the microscope on the digital sensor of the camera. An important optical-mechanical discrepancy was observed and discussed during the stage of the experimental design. It was also found that the 0.5x reduction lens has a near 60 percent field of view (FOV) that is seen by the human eye through the eyepiece. It is a physical limitation due to the nonconformance of the digital sensor size by the focal tattoo factors of the lens adapter. Even though this discrepancy also leads to a decrease in the capture area per single image, the clarity and diagnostic fidelity in the 60% area is good. In order to make certain that this physical factor does not result in the loss of diagnostic data, the system structure has adopted the multi-field acquisition scheme and computational summation, as shown in Figure 3.

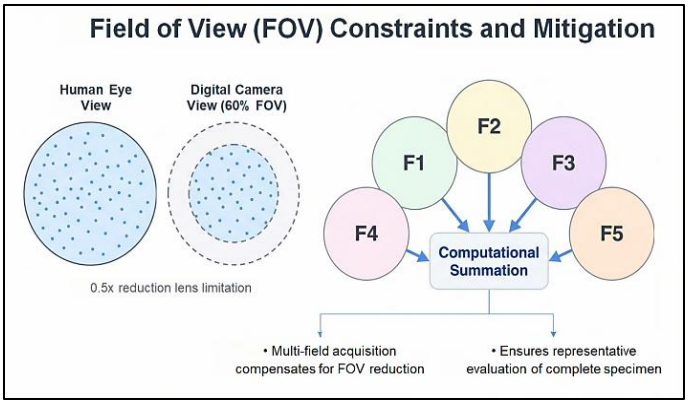

Fig. 3. Multi-field acquisition scheme illustrating the five-field (F1–F5) sampling strategy used to overcome the 60% FOV hardware limitation.

which are able to restore a representative evaluation of the complete specimen. In line with the hardware and imaging elements, the Computational Processing Unit, which is usually a standard personal computer or laptop, is the one that should be supported. The system is deliberately crafted to be computationally modest so as to focus on portability, low cost and simple implementation in normal laboratory settings. This is the processing unit of the platform and it contains the software interface and handles the high speed data rate of the digital camera. The processing unit carries out a number of critical roles prior to transmission of the data to be analyzed. It deals with real-time image capture, where the user could view the microscopic field on the screen. It also performs normalization of resolutions, noises as well as enhancement of the structure to make sure that there is standardization of visual input, irrespective of the kind of microscope brand or lighting conditions applied. Moreover, the processing unit is a secure gateway; the role of the de-identification of microscopic imagery will be trusted to ensure patient confidentiality and then the transmission of this anonymized information via encrypted API tunnels to the clouded intelligence layer. The integration is what makes the information flow between the physical slide and the analytical engine seamless without making the clinical safety or information integrity depend on any particular step of the diagnostic process.

2.2 Image Acquisition and Digital Pre-processing Protocol:

Digitization of a physical biological specimen to create a high-fidelity digital format that can be analyzed with artificial intelligence is an important step in the MicroScan AI workflow. The given methodology is particularly designed in such a way that the visual data obtained should be both as high-resolution as possible, and statistically representative of the overall clinical sample. The acquisition and processing algorithm can be broken down into systematic sampling strategy and strict digital enhancement pipeline.

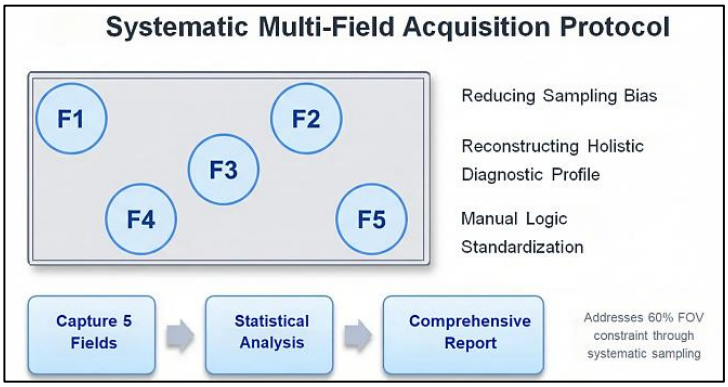

Fig. 4. Image acquisition and digital pre-processing pipeline showing the systematic multi-field capture and normalization steps.

The major issue associated with the digital microscopy is that a single captured frame should offer sufficient diagnostic data to represent the entire specimen. In order to overcome the above-mentioned 60 percent Field-of-View (FOV) constraint on the system due to the 0.5x reduction lens, and to recreate the careful scanning of a human laboratory specialist, the system uses a Systematic Multi-Field Acquisition Protocol. The system is coded to record five independent and discreet microscopic fields, labeled F1, F2, F3, F4, and F5, of each individual urine or stool sample as opposed to using a localized snapshot. As shown in Figure 4.

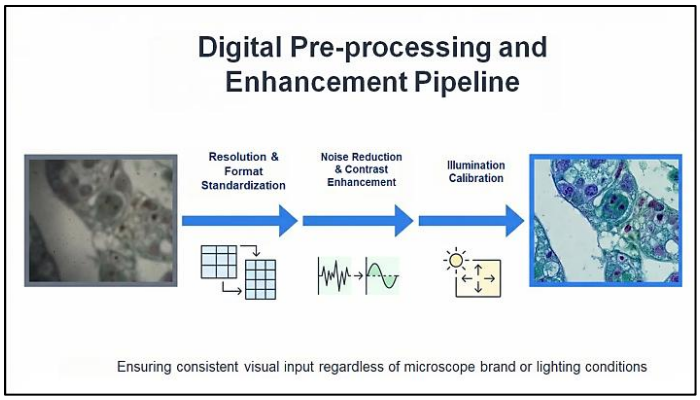

Fig. 5. Illustration of the three diagnostic functions of the multi-field strategy: reducing sampling bias, reconstructing a holistic diagnostic profile, and standardizing manual logic.

The three basic diagnostic functions served by this strategy include: first, Reducing Sampling Bias, since biological structures like parasites, ova, or cellular casts do not tend to be evenly spread on a glass slide, by obtaining five fields the system has a high chance of detecting any localized pathological abnormalities, and a lesser chance of being misled by blank areas. Second, Reconstructing a Holistic Diagnostic Profile, in which the system essentially fuses information about five partially overlapping or completely different areas, the system computes a diagnostic assessment

effectively compensating the physical loss of field-of-view, so that the final report relies on a cumulative assessment, as opposed to a solitary observation. Third, Manual Logic Standardization, because this protocol is reflective of the clinical standard that has been in place in which a technologist is required to scan various fields before stating the absence or presence of certain microscopic components. After the five raw images are acquired through the hardware interface, it is sent into the Processing Layer, which exists on the local computational unit. Prior to the transmission of these images to the cloud intelligence layer, these images have to pass through a sequence of technical procedures of normalization so that the same analytical outcome is attained in various laboratory settings. The pre-processing pipeline encompasses Resolution and Format Standardization [26], which the system is used to resize and format the captured images to fit the exact architectural needs of the multimodal Large Language Models (LLMs) without any harm to the integrity of fine morphological information. It also encompasses Noise Reduction and Contrast Enhancement where mathematical filters are used to deal with electronic noise and optical artifacts which can occur due to changes in microscope light. Such an improvement is essential to bring out the internal textures of parasites and the delicate edges of hyaline casts, which would otherwise be lost in debris in the background. In addition, Illumination Calibration is done, which automatically provides the system with variations in brightness, so that the engines of AI get used to a commonized visual input rather than the individual lighting arrangement of the optical microscope being operated. As shown in Figure 5.

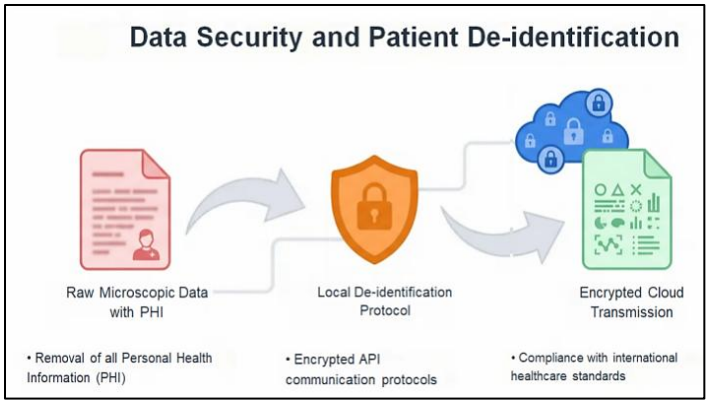

Fig. 6. Data security and medical ethics protocol showing the de-identification and encrypted API transmission pipeline.

Being a cloud-based diagnostic device, MicroScan AI ranks Data Security and Medical Ethics at the forefront. The conversion of data between the local lab and the intelligence layer is regulated by a stringent security measure that is aimed to preserve the privacy of the patients and use the advanced AI resources. An important binding of this protocol is the De-identification Process; prior to transmitting any image, the system is used to remove all the Personal Health Information (PHI) and metadata that may identify the patient. The local unit only permits the anonymized microscopic visual data to exit the unit. This information is then sent by encrypted and secure API with access to the

specified AI analytical engines (ChatGPT-4o, Gemini or Claude). This coded communication keeps the information safe against unauthorized access and it is in compliance with the international standards in regards to digital healthcare and patient data protection. This bi-layered strategy, i.e. local anonymization with cloud-level encryption, is the guarantee that the system is intelligent and as safe as it is smart. As shown in Figure 6.

2.3 AI-Driven Analytical Framework and Specialized Prompt Engineering:

MicroScan AI framework The intelligence level of the MicroScan is driven by the state-of-the-art Multimodal Large Language Models (LLMs) [27], such as ChatGPT-4o by OpenAI, Gemini 1.5 Pro by Google and Claude 3.5 Sonnet by Anthropic. They were chosen to be used due to their advanced vision-language potentials that enable them to do high-level morphological reasoning with microscopic imagery without such extensive task-specific training. These multimodal engines have zero-shot and few-shot learning, unlike more traditional convolutional neural networks (CNNs), which need very large labeled datasets in order to discover pathological components using their internal understanding of medical morphology. These particular models are selected because they provide a strong and varied analytical space, in which each individual architecture, including the reasoning capabilities of ChatGPT, the large context window of Gemini, and the accuracy of Claude, can be used to validate the clinical use of these models.

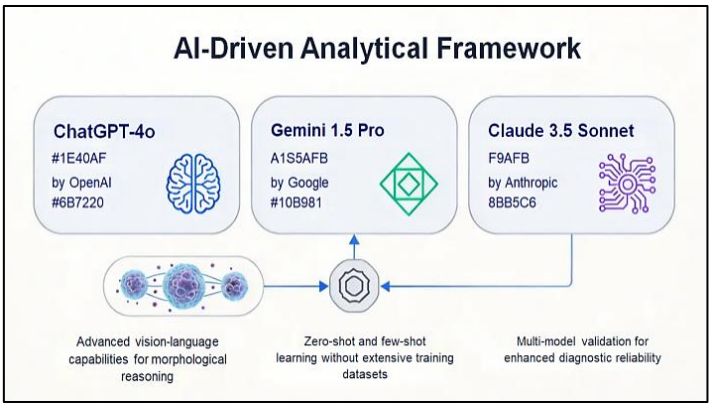

Fig. 7. Overview of the three multimodal LLMs selected for the MicroScan AI analytical framework: ChatGPT-4o, Gemini 1.5 Pro, and Claude 3.5 Sonnet.

In order to achieve maximum accuracy in diagnosis and clinical relevance, the system will utilize the MicroScan AI Systematic Prompting Engine, which is a specialized system of interaction with the AI layers. The prompt engineering plan will make the LLMs have a clear clinical setting, which will turn them into specialized virtual pathologists. The prompting architecture is composed of four functional elements: Role Definition, which teaches the model to perform as a specialist in clinical laboratory work; Task Specification, which details what analysis is required, i.e. whether the analysis is an analysis of urinalyses or an analysis of fecalyses; Morphological Recognition Instructions, which is a specific directive regarding the identification of erythrocytes, leukocytes, epithelial cells, casts,

crystals, and other life stage forms of parasites (e.g. cysts, ova, etc.). This is a structured output as shown in Figure 8.

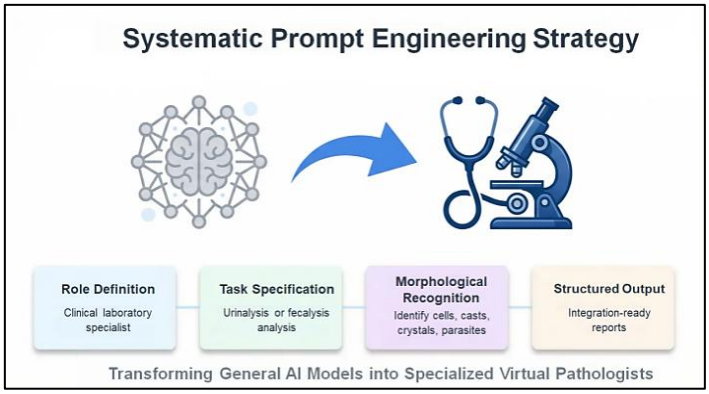

Fig. 8. Structured output format required by the computational aggregation step and laboratory information system (LIS) integration.

Required by the next step of computational aggregation and the ability to seamlessly incorporate the findings of the AI into a patient report or a laboratory information system (LIS). One of the fundamental innovations of the MicroScan AI architecture is that it is a Clinical Decision-Support Tool (CDST). The system is not created to eliminate the human technologist but support his or her functions with a secondary, highly consistent analytical opinion. This is done by a Multi-Model Validation Strategy in which the results of the various AI engines are compared to each other so that the results are clinically reliable. The system compares the confidence scores of each model and notifies about the substantial difference to be checked by human resources. The analytical framework offered by the AI offers structured diagnostic information and confidence rates, which eliminates the cognitive load on laboratory staff and can be used as an effective quality assurance tool, especially in a large-volume laboratory environment, where human exhaustion is a contributing factor. This combination makes sure that each microscopic field has been examined in the same degree of rigorous morphological examination irrespective of the time of day as well as the necessarily heavy workload of the human operator.

2.4 Computational Aggregation and Statistical Methodology:

The MicroScan AI system depends largely on the analytical integrity, which is required to synthesize several data points into one, clinically actionable diagnostic report. This means that, since the hardware layout of the system, namely the 0.5× reduction lens, is only able to capture about 60 per cent of the field of view as viewed by a human specialist, the system must include a more complicated computing aggregation layer; otherwise representative sampling cannot be guaranteed. The approach to classification of images is taken a step further as it utilizes a Counting-Based Aggregation approach model which approximates the cumulative observation procedure of trained laboratory experts. The system statistically addresses the possibility of missing localized pathological features by performing

a five-independent fields of view analysis of each specimen and offers a solid quantitative and qualitative analysis of the sample. To obtain a precise quantification of diagnostic elements (e.g. the number of Red Blood Cells (RBCs) and White Blood Cells (WBCs) per High Power Field (HPF)) the system uses a standardized protocol of arithmetic averaging. At the acquisition stage, the artificial intelligence engine examines five different microscopic fields (F1, F2, F3, F4 and F5) separately. In order to get the final reported value ($\bar{C}$) of the individual counts of these five fields, the system uses the arithmetic mean of the resulting counts. This procedure makes sure that the result of the diagnostic should not be biased with the unequal distribution of the cellular components on the glass slide. The mathematical model of this aggregation is as follows:

$$\bar{C} = (1/n)\, \Sigma\, C_i \quad (1)$$

In this model, C_i denotes the numeric number of a certain microscopic constituent found in a single field (i), and n denotes the number of fields under consideration, which is denoted as 5 in this paper. As shown in Figure 9.

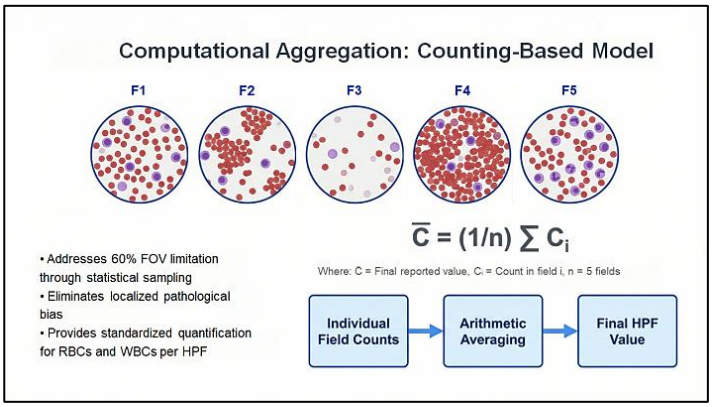

Fig. 9. Counting-based aggregation model illustrating the arithmetic mean calculation across five microscopic fields (F1–F5).

The approach correlates the output of the system with the international laboratory reporting requirements, where an average number of counts on a number of fields will give a more valid reflection on the clinical condition of a patient compared to one localized observation. Besides numerical values, several microscopic observations are described by semi-quantitative values including Trace, Few (+), Moderate (++), many (+++/++++). The different aggregation logic is needed in these parameters such as the presence of bacteria, yeast, epithelial cells, and different kinds of urinary casts. The system uses a Consensus-Based Grading Rule to eliminate the differences across fields. The reasoning behind it is based on a majority-vote concept when the grade that is most frequently displayed in the five fields is chosen as the main outcome. Nevertheless, to add to the clinical safety and minimize the risk of not underestimating potentially important pathological results, the system is programmed with a Conservative Bias protocol. In case the AI recognises two

neighboring grades (such as in two subjects plus and in three subjects plus plus, or a draw between neighbor grades), the system will be configured to report the better grade. As shown in Figure 10.

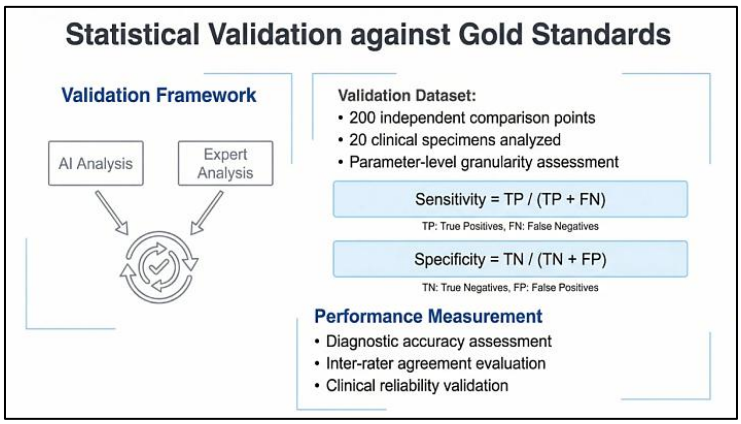

Fig. 10. Conservative Bias protocol logic ensuring the higher adjacent grade is reported in borderline cases to maximize diagnostic sensitivity.

This is to provide high diagnostic sensitivity especially to such elements as parasitic ova or hyaline casts where under-reporting may cause them to delay in receiving a diagnosis or treatment. In order to strongly assess the analytical performance of MicroScan AI, the system was assessed against a "Gold Standard" based on the performance of experienced laboratory personnel that appraised the very images that were digitized. The validation was carried out at a parameter-level granularity, which offered 200 comparison points independent of each other in 20 clinical specimens. This strategy has the statistical robustness even with a designated sample. The system diagnostic performance was measured with the help of the following statistical values: Sensitivity characterizes the system capability to recognize the presence of a pathological finding (True Positives). It is obtained by the formula:

$$Sensitivity = TP / (TP + FN) \quad (2)$$

where TP is the True Positives and FN is the False Negatives. Specificity gauges how the system can detect the non-occurrence of a finding or normal finding accurately (True Negatives):

$$Specificity = TN / (TN + FP) \quad (3)$$

where TN is True Negatives and FP is False Positives. As shown in Figure 11.

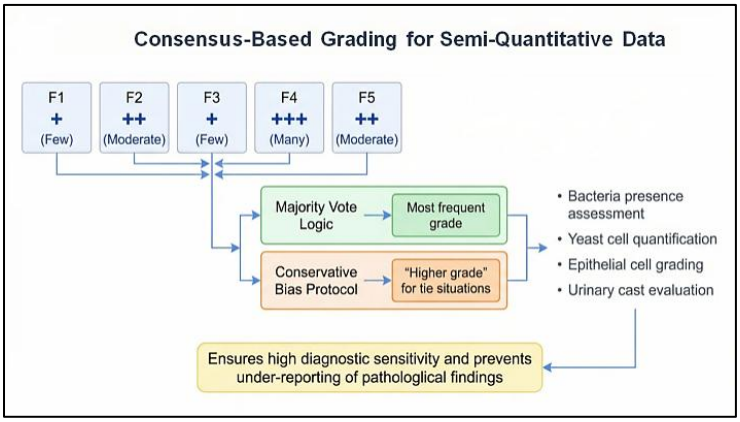

Fig. 11. Statistical validation framework comparing MicroScan AI output against the human expert Gold Standard across 200 diagnostic parameters.

The indicators of the reliability of the given system in the most prominent way are the level of correlation between the results of the AI and human experts. In order to measure this, Cohen's Kappa Coefficient (κ) is used as a statistical measure of inter-rater agreement that is used in the system which takes into consideration the fact that the agreement may be random. The Kappa coefficient is calculated as follows:

$$\kappa = (P_o - P_e) / (1 - P_e) \quad (4)$$

In this expression, P_o is the proportion of agreement seen between the AI and the human specialist and P_e is the hypothetically possible probability of chance agreement. In clinical validation, MicroScan AI had a total agreement rate of 97% ($P_o = 0.97$), which gave it a κ value of 0.94. With the approved diagnostic interpretation scales, 0.94 is considered to be in the category of Almost Perfect Agreement. A finer examination of the remaining 3% error showed that the remaining discrepancies were entirely on the side of the "Adjacent Grade Discrepancies" — where the objective numerical counting by the AI activated a subjective visual estimate of the human observer. Notably, there were no instances of categorical failures since the system was not missing any pathological parts or parasites as shown in Figure 12. This strict statistical model proves that MicroScan AI is a very safe decision support tool that can provide a regular clinical setting with consistent and reliable microscopic analysis.

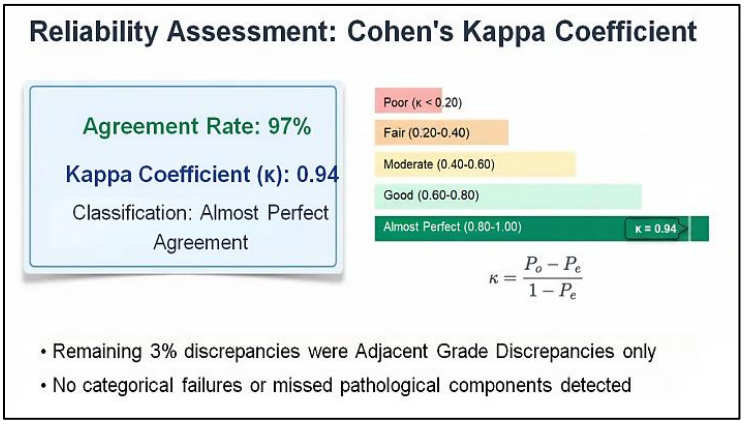

Fig. 12. Summary of the 3% discrepancy analysis confirming all errors were Adjacent Grade Discrepancies with zero categorical failures.

3. Results

3.1 Diagnostic Concordance:

MicroScan AI was experimentally validated and revealed a remarkably high rate of analytical performance with over 97 per cent overall agreement rate over 200 independent diagnostic comparison points as illustrated in Table 1. The Kappa coefficient of the recorded Cohen is especially noteworthy, as it classifies the inference between the AI-powered system and the lab personnel with real-life experience as the Almost Perfect Agreement. The most notable result of this study is that the multimodal analytical engines of the system, in this case, the primary validating engine ChatGPT-4o may reproduce the interpretative reasoning of human specialists with the highest precision. The system was able to find all the cases of parasitic forms of life (cysts, eggs, or trophozoites) and pathological elements of the images (urinary cast and crystalline structure). This proves that the pattern-recognition abilities of the AI are good enough to sever essential clinical signals with no false negative detection and supports the system as an effective decision-support tool.

Table 1. Overall Diagnostic Agreement Across 20 Clinical Samples

Sample ID	Specimen Type	Parameters Compared	Matches	Mismatches	Agreement (%)	Notes on Discrepancy
U1	Urine	10	10	0	100%	Full Concordance
U2	Urine	10	9	1	90%	Adjacent Grade (Few vs Moderate)
U3	Urine	10	10	0	100%	Full Concordance
U4	Urine	10	10	0	100%	Full Concordance
U5	Urine	10	9	1	90%	Borderline Numerical Threshold
U6	Urine	10	10	0	100%	Full Concordance
U7	Urine	10	10	0	100%	Full Concordance
U8	Urine	10	10	0	100%	Full Concordance

Sample ID	Specimen Type	Parameters Compared	Matches	Mismatches	Agreement (%)	Notes on Discrepancy
U9	Urine	10	9	1	90%	Adjacent Grade Discrepancy
U10	Urine	10	10	0	100%	Full Concordance
S1	Stool	10	10	0	100%	Full Concordance
S2	Stool	10	9	1	90%	Threshold Sensitivity
S3	Stool	10	10	0	100%	Full Concordance
S4	Stool	10	10	0	100%	Full Concordance
S5	Stool	10	9	1	90%	Borderline Count Logic
S6	Stool	10	10	0	100%	Full Concordance
S7	Stool	10	10	0	100%	Full Concordance
S8	Stool	10	10	0	100%	Full Concordance
S9	Stool	10	9	1	90%	Adjacent Grade Discrepancy
S10	Stool	10	10	0	100%	Full Concordance
Total	—	**200**	**194**	**6**	**97%**	**Cohen's Kappa: 0.94**

3.2 Diagnostic Disparities:

The 3% difference between AI and human vision (6 misfits of 200 parameters) offers an in-depth understanding of how artificial intelligence and human senses work. These errors were only classified as Adjacent Grade Discrepancies which happen at borderline quantitative levels and not categorical detection errors. There are two different interpretative frameworks: Objective Numerical Thresholding: The MicroScan AI system follows a strict counting logic and hard mathematical boundaries specified in their clinical prompts. As an example, a field of 11 Red Blood Cell (RBCs), the system determines the field to be objectively classified as moderate (++) according to the standardized 10–20 cells range as presented in Table 2. Subjective Human Heuristics: Human reviewers tend to use visual cues and subjective estimations, which restricts them to sorting borderline cases into the lower or higher grade based on perceived sparse distribution. This inconsistency underscores the fact that the AI is more mathematically inflexible, whereas the returned variance is limited to the intensity grading as opposed to misidentification. The system has not compromised the performance because there was no major pathological structure that was not properly observed.

Table 2. Semi-Quantitative Grading Thresholds for RBC Count per HPF

RBC Count per HPF	AI Classification	Symbol	Mathematical Rule Applied
0	None	−	Count = 0
1–5	Mild	+	$1 \leq \text{Count} \leq 5$
6–10	Few	+	$6 \leq \text{Count} \leq 10$
11–20	Moderate	++	$11 \leq \text{Count} \leq 20$
21–50	Many	+++	$21 \leq \text{Count} \leq 50$
>50	Numerous	++++	Count > 50

3.3 Hardware Constraint Mitigation with Software Strategy:

The findings affirm that the main constraint in the system is optical-mechanical not the algorithmic one. The reduction lens with the size of 0.5x and thus reduced the captured field of view (FOV) to about 60 percent of human observation, posed a threat in the first place to quantitative accuracy. Nevertheless, the application of the Five-Field (F1–F5) Acquisition Strategy and Counting-Based Aggregation methodology were highly successful in addressing this drawback. The system was able to produce analytical results that are, in effect, comparable to full-field human microscopy by rebuilding a representative diagnostic profile using the arithmetic mean of more than one field. It proves that cost effective hardware expansion in combination with ordered computational aggregation can effectively overcome the gap between analog equipment and digital intelligence without losing diagnostic integrity as indicated in Table 3.

Table 3. Statistical Performance Summary (200 Comparison Points)

Performance Metric	Value / Achievement	Clinical Significance
Overall Agreement	97.0%	High analytical concordance
Cohen's Kappa (κ)	0.94	Almost Perfect Agreement
Categorical Failure Rate	0.0%	No parasites or pathogens missed
Sensitivity	High (100% for pathogens)	Reliable for disease detection
Specificity	High (100% for negative samples)	Low risk of false positives
Confidence Interval	95%	Statistically robust result range
Discrepancy Nature	100% Adjacent Grade	Errors limited to borderline estimates

3.4 Clinical Safety and the Conservative Bias Logic:

The effects of the Consensus-Based Aggregation Rule on clinical safety should also be discussed. To achieve this, the system is specially coded with a logic of Conservative Bias that will revert to the stronger of the two adjacent grades in case the two grades made equal frequencies in the five fields evaluated. Although this reasoning led to some of the documented discrepancies, where the AI will report a higher grade than the human specialist, it is a purposely designed aspect of methodology that is focused on being sensitive in cases of the borderline, meaning that potentially pathological factors will be actively identified and subjected to human consideration. The system will give a layer of transparency by presenting a Confidence Score with each output, warning the laboratory personnel of cases that are complicated or marginal. The interpretative framework will make sure that the MicroScan AI will improve diagnostic consistency but adhere to the principle of maintaining the human-in-the-loop principle as the ultimate diagnostic power. The calculated criteria are indicated in Table 4.

Table 4. Representative Analysis of a Single Clinical Specimen

Parameter	Human Expert Result	AI Result	Agreement Status
RBCs (Count)	6	6	Match
WBCs (Grading)	++	++	Match
Epithelial Cells	+	+	Match
Pus Cells	+	+	Match

Parameter	Human Expert Result	AI Result	Agreement Status
Bacteria	++	++	Match
Yeast	Negative	Negative	Match
Casts	Negative	Negative	Match
Mucus Threads	+	+	Match
Crystals	Negative	Negative	Match
Parasites / Ova	Negative	Negative	Match

4. Conclusion

The creation and testing of an intelligent system, MicroScan AI, hopefully demonstrate that a low-cost, adaptable system can be used to modernize the routine laboratory diagnostics, by combining standard optical microscopes with digital imaging and multimodal Large Language Models (LLMs), namely ChatGPT-4o, which will serve as a scalable solution to the problem of filling the gap between manual microscopy and automated digital pathology. High analytical accuracy is the most important findings of this work because the system reported a 97 percent overall agreement rate based on 200 independent diagnostic parameters after being applied to 20 cases of clinical samples, and statistical reliability because the Cohen kappa coefficient was 0.94, which indicates the presence of the "Almost Perfect Agreement" of the AI-based framework and the human specialists with extensive clinical experience. In addition, the system was pathologically safe as it reported a 0-percent categorical failure rate, was able to detect all parasitic life-stages and pathological components without any significant finding being missed, and offered a methodological compensation to the optical-mechanical limitation where the 0.5x lens only observed 60 percent of the field of view by executing a five-field aggregation plan and arithmetic averaging. Specialized Prompt Engineering and Raw JSON outputs are also used, in order to support clinical integration, enabling the deterministic parsing of laboratory interfaces, and Confidence Scores provide for the mandatory human review of marginal cases. Overall, MicroScan AI is an effective clinical decision-support system that creates less dependence on operators, promotes the consistency of diagnosis, and can train novice technologists.

References

[1] S. Haymond and C. McCudden, "Rise of the Machines: Artificial Intelligence and the Clinical Laboratory.," J. Appl. Lab. Med., 2021. [Online]. Available: https://academic.oup.com/jalm/article/6/6/1640/6348035

[2] P. Moretti, R. Franchi, T. M. Poluzzi, and S. Paltrinieri, "Analytical variability and uncertainty in canine leukocyte ratios obtained with manual counts.," Vet. Rec., 2022. [Online]. Available: https://bvajournals.onlinelibrary.wiley.com/doi/10.1002/vetr.1628

[3] H. Xie, Y. Jia, and S. Liu, "Integration of artificial intelligence in clinical laboratory medicine: Advancements and challenges," Interdiscip. Med., 2024. [Online]. Available: https://onlinelibrary.wiley.com/doi/10.1002/INMD.20230056

[4] A. Rahman, C. L. Cheng, R. Salim, H. G. Di Shen, W. M. Gallagher, and J. Iqbal, "Digital pathology and AI: enhancing molecular diagnostics in low- and middle-income countries," Expert Rev. Mol. Diagn., vol. 25, no. 12, pp. 859–867, 2025, doi: 10.1080/14737159.2025.2581687.

[5] A. Molani et al., "Advances in Portable Optical Microscopy Using Cloud Technologies and Artificial Intelligence for Medical Applications," Sensors, vol. 24, no. 20, 2024, doi: 10.3390/s24206682.

[6] A. Mullan and A. Marsh, "Choosing the Best Camera for fluorescence Microscopy," J. R. Microsc. Soc., pp. 16–22, 2019, doi: 10.22443/rms.inf.1.172.

[7] I. Kim, K. Kang, Y. Song, and T.-J. Kim, "Application of Artificial Intelligence in Pathology: Trends and Challenges," Diagnostics, vol. 12, no. 11, 2022, doi: 10.3390/diagnostics12112794.

[8] R. Liu, W. Dai, T. Wu, M. Wang, S. Wan, and J. Liu, "AIMIC: Deep Learning for Microscopic Image Classification," Comput. Methods Programs Biomed., vol. 226, p. 107162, 2022, doi: https://doi.org/10.1016/j.cmpb.2022.107162.

[9] Y. Rivenson, Z. Göröcs, H. Günaydin, Y. Zhang, H. Wang, and A. Ozcan, "Deep learning microscopy," Optica, vol. 4, no. 11, pp. 1437–1443, 2017, doi: 10.1364/OPTICA.4.001437.

[10] J. von Bahr, A. Suutala, V. Diwan, A. Mårtensson, J. Lundin, and N. Linder, "AI-Supported Digital Microscopy Diagnostics in Primary Health Care Laboratories: Scoping Review," J Med Internet Res, vol. 28, p. e78500, 2026, doi: 10.2196/78500.

[11] S. K. Mondal, M. Islam, and M. S. U. Yusuf, "An artificial intelligence-based approach for human parasite egg segmentation and classification," Healthc. Anal., vol. 8, p. 100432, 2025, doi: https://doi.org/10.1016/j.health.2025.100432.

[12] K. M. Naing et al., "Automatic recognition of parasitic products in stool examination using object detection approach," PeerJ Comput. Sci., vol. 8, p. e1065, 2022, doi: 10.7717/peerj-cs.1065.

[13] M. Li, Q. Gao, and T. Yu, "Kappa statistic considerations in evaluating inter-rater reliability between two raters: which, when and context matters," pp. 1–5, 2023.

[14] M. Ji, G. Z. Genchev, H. Huang, T. Xu, H. Lu, and G. Yu, "Evaluation Framework for Successful Artificial Intelligence–Enabled Clinical Decision Support Systems: Mixed Methods Study," J Med Internet Res, vol. 23, no. 6, p. e25929, 2021, doi: 10.2196/25929.

[15] J. Cadamuro et al., Clin. Chem. Lab. Med., vol. 63, no. 4, pp. 692–703, 2025, doi: 10.1515/cclm-2024-1016.

[16] H. Go, "Digital Pathology and Artificial Intelligence Applications in Pathology," vol. 10, no. 2, pp. 76–82, 2022.

[17] M. Sonntagbauer, M. Haar, and S. Kluge, "[Artificial intelligence: How will ChatGPT and other AI applications change our everyday medical practice?].," Med. Klin. Intensivmed. Notfmed., vol. 118, no. 5, pp. 366–371, Jun. 2023, doi: 10.1007/s00063-023-01019-6.

[18] R. Kaczmarczyk, T. Wilhelm, R. Martin, and J. Roos, "Evaluating multimodal AI in medical diagnostics," npj Digit. Med., vol. 7, 2024, doi: 10.1038/s41746-024-01208-3.

[19] M. Harfouche et al., "Imaging across multiple spatial scales with the multi-camera array microscope," Optica, vol. 10, no. 4, pp. 471–480, 2023, doi: 10.1364/OPTICA.478010.

[20] W.-C. Chen, C.-C. Chang, and Y. E. Lin, "Pulmonary Tuberculosis Diagnosis Using an Intelligent Microscopy Scanner and Image Recognition Model for Improved Acid-Fast Bacilli Detection in Smears," Microorganisms, 2024. [Online]. Available: https://www.mdpi.com/2076-2607/12/8/1734

[21] E. Clarke et al., "Faster than light (microscopy): superiority of digital pathology over microscopy for assessment of immunohistochemistry," J. Clin. Pathol., vol. 76, no. 5, pp. 333–338, 2023, doi: 10.1136/jclinpath-2021-207961.

[22] K. Basak, "Whole Slide Images in Artificial Intelligence Applications in Digital Pathology: Challenges and Pitfalls," pp. 101–108, 2023, doi: 10.5146/tjpath.2023.01601.

[23] L. Budach et al., "The Effects of Data Quality on Machine Learning Performance," 2022. [Online]. Available: https://www.semanticscholar.org/paper/b70226c67cfd7225a18f9c9efc61d1344584b507

[24] K. Nurzynska, M. Strzelecki, A. Piórkowski, and R. Obuchowicz, "AI in Medical Imaging and Image Processing," J. Clin. Med., vol. 14, no. 12, 2025, doi: 10.3390/jcm14124153.

[25] C. Liu, D. Li, and P. Huang, "ISE-YOLO: Improved Squeeze-and-Excitation Attention Module based YOLO for Blood Cells Detection," 2021 IEEE Int. Conf. Big Data (Big Data), 2021. [Online]. Available: https://doi.org/10.1109/bigdata52589.2021.9672069

[26] T. Islam, M. S. Hafiz, J. Jim, M. Kabir, and M. Ph.D., "A systematic review of deep learning data augmentation in medical imaging: Recent advances and future research directions," Healthc. Anal., vol. 5, p. 100340, 2024, doi: 10.1016/j.health.2024.100340.

[27] B. D. Simon, K. B. Ozyoruk, D. G. Gelikman, S. A. Harmon, and B. Türkbey, "The future of multimodal artificial intelligence models for integrating imaging and clinical metadata: a narrative review.," Diagn. Interv. Radiol., vol. 31, no. 4, pp. 303–312, Jul. 2025, doi: 10.4274/dir.2024.242631.